Chemical Science

ROYAL SOCIETY OF CHEMISTRY

EDGE ARTICLE

View Article Online
View Journal | View Issue

Cite this: *Chem. Sci.*, 2021, **12**, 9726

All publication charges for this article have been paid for by the Royal Society of Chemistry

Received 6th May 2021
Accepted 16th June 2021

DOI: 10.1039/d1sc02498a

rsc.li/chemical-science

Transfer of polyantimony units†

Veronika Heinl, Andreas E. Seitz, Gábor Balázs, Michael Seidl and Manfred Scheer *

Transfer reagents are useful tools in chemistry to access metastable compounds. The reaction of $[Cp''_2ZrCl_2]$ with $KSb(SiMe_3)_2$ leads to the formation of the novel polyantimony triple decker complex $[(Cp''Zr)_2(\mu,\eta^{1:1:1:1:1:1}\text{-}Sb_6)]$ (**1**, Cp″ = 1,3-di-tertbutyl-cyclopentadienyl), containing a chair-like Sb_6^{6-} ligand. Compound **1** represents a valuable transfer reagent to form novel antimony ligand complexes. Thus, the reaction of **1** with Cp^R-substituted transition metal halides of nickel, cobalt and iron leads to the formation of a variety of novel Sb_n ligand complexes, such as the cubane-like compounds $[(Cp'''Ni)_4(\mu_3\text{-}Sb)_4]$ (**2**) and $[(Cp'''Co)_4(\mu_3\text{-}Sb_4)]$ (**3a**) or the complexes $[(Cp^{Bn}Co)_3(\mu_3\text{-}Sb)_2]$ (**4**) and $[(Cp'''Fe)_3(\mu_3\text{-}Sb)_2]$ (**5**), representing a trigonal bipyramidal structure. Moreover, beside the transfer of Sb_1 units, also the complete entity can be transferred as seen in the iron complex $[(Cp'''Fe)_3(\mu_3,\eta^{4:4:4}\text{-}Sb_6)]$ (**6**). DFT calculations shed light on the bonding situation of the products.

Introduction

The reactivity of polypnictogen ligand complexes is an active field of chemical research, which resulted in numerous novel E_n complexes (E = P, As, Sb).[1,2] Especially for phosphorus and arsenic, a large variety of examples have been synthesized so far, usually by employing white phosphorus or yellow arsenic in the reaction with transition metal or main group compounds.[3–6] In contrast, the number of polyantimony ligand complexes is very limited and, therefore, their chemistry was far less investigated.[7] Reasons for this can be attributed to various challenges such as the sensitivity of antimony-containing compounds towards light, the weak Sb–Sb bonding[8] and especially the lack of suitable antimony sources. Since Sb_4 is only known in the gas phase or under special conditions, *e.g.* trapped in a solid neon matrix,[9] grey antimony, Zintl ions,[10] organo-substituted Sb precursors[11] and quite simply $SbCl_3$ (ref. 12–14) and its derivatives were used as starting materials. In the 1970s, the first Sb_n ligand complex $[\{Co(CO)_3\}_4(\mu_3\text{-}Sb)_4]$ was published by Dahl *et al.* by the reaction of $Co(OAc)_2\cdot H_2O$ with $SbCl_3$ as antimony source (**I**, Fig. 1).[12] Even in the case of the complexes $[Sb_2\{W(CO)_5\}_3]$[13] (**II**) and $[\{LGa(NMe_2)\}_2(\mu,\eta^{1:1}\text{-}Sb_4)]$[14] (**III**), $SbCl_3$ and $Sb(NMe_2)_3$ are used as precursors (Fig. 1, L = $HC[C(Me)N(2,6\text{-}C_6H_3{}^iPr_2)]_2$).

The most commonly applied antimony sources, to build polyantimony ligand complexes or main group compounds, are neutral organo-substituted antimony units such as R_4Sb_4 (R = Cp*, ^{t}Bu; Cp* = η^1-C_5Me_5)[15–17] and R'_4Sb_2 (R′ = Me, Et).[18] Rösler *et al.* succeeded in the synthesis of the molybdenum complexes $[\{CpMo(CO)_2\}_2(\mu,\eta^2\text{-}Sb_2)]$ (**IV**) and $[Cp'''Mo(\mu,\eta^{5:5}\text{-}Sb_5)MoCp^R]$ (**V**, Fig. 1; Cp‴ = η^5-$C_5H_2{}^tBu_3$, Cp^R = η^5-$C_5H_2{}^tBu_2Me$) by thermolysis of $^tBu_4Sb_4$ with $[CpMo(CO)_3]_2$ and $[Cp'''Mo(CO)_3CH_3]$, respectively.[15,16] **V** represents the first triple-decker sandwich complex containing a *cyclo*-Sb_5 middle deck. Interestingly, one *t*Bu group of the Cp‴ ligand is degraded to a methyl group during the thermolytic reaction.[16]

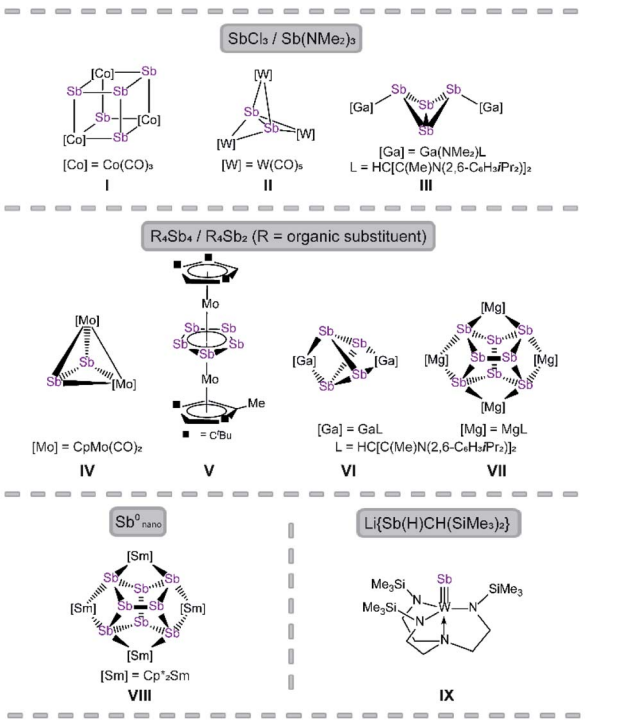

Fig. 1 Selected examples of Sb_n ligand complexes.

Institut für Anorganische Chemie, Universität Regensburg, 93040 Regensburg, Germany. E-mail: Manfred.Scheer@ur.de; Web: https://www.uni-regensburg.de/chemie-pharmazie/anorganische-chemie-scheer/

† Electronic supplementary information (ESI) available. CCDC 2079755–2079760. For ESI and crystallographic data in CIF or other electronic format see DOI: 10.1039/d1sc02498a

Recently, the chemistry of the polyantimony main group compounds has experienced a revival[5,19] especially by the introduction of the nacnac ligand in combination with Mg and Ga (*i.e.* LMg and LGa) in this field. In addition to the aforementioned compound **III**, $[(LGa)_2(\mu,\eta^{2:2}\text{-}Sb_4)]$[17] (**VI**) and $[(LMg)_4(\mu_4,\eta^{2:2:2:2}\text{-}Sb_8)]$[18] (**VII**) are interesting representatives made of organo-substituted antimony precursors. **VI** is formed by the reaction of LGa with $Cp^*_4Sb_4$ *via* reductive elimination of decamethyl-dihydrofulvalene Cp^*_2 and oxidative addition of LGa to the Sb_4 subunit.[17] To form **VII**, the reducing agent $[(LMg)_2]$ was used to initiate the cleavage of the Sb–C bonds in R'_4Sb_2.[18] Another possibility to build polyantimony ligand complexes was shown by P. Roesky *et al.* by the usage of Sb^0 nanoparticles in the thermolysis reaction with $[Cp^*_2Sm]$, leading to the formation of the f-element polystibide $[(Cp^*_2\text{-}Sm)(\mu_4,\eta^{2:2:2:2}\text{-}Sb_8)]$ (**VIII**), similar to **VII**.[20] Also, our group is interested in the generation of Sb_n ligand complexes with unprecedented structural motifs. For instance, we succeeded in the synthesis of $[(N_3N)WSb]$ (**VI**, N_3N = tren = $N(CH_2CH_2NSiMe_3)_3$) which possesses a first tungsten antimony triple bond compound.[21] Here, a lithium antimonide salt was used as Sb_1 source. Due to the lack of suitable antimony precursors, the access to polyantimony compounds is strongly limited (*vide supra*), in principle due to their instability. The classical synthetic procedures, *i.e.* thermolysis or photolysis, lead in most of the cases to gray antimony.

Besides the usual synthetic pathways such as thermolysis, photolysis or reactions with unsaturated fragments, the transfer of E_n units constitutes a promising procedure for the synthesis of metastable E_n ligand complexes, since such reactions proceed under mild conditions and enable the formation of compounds that are not accessible by other means.[4,6,22] A prominent product of such a transfer reaction is the synthesis of AsP_3, reported by Cummins *et al.*, where a P_3^{3-} unit was transferred from a niobium complex to $AsCl_3$.[23] As_n units were also transferred from the zirconium complexes $[Cp''_2Zr(\mu,\eta^{1:1}\text{-}E_4)]$ (E = P, As) to LSi, leading to the formation of the inorganic benzene derivatives $L_3Si_3E_3$ (E = P, As; L = $PhC(N^tBu)_2$).[24] Moreover, this approach was extended to transition metals.[25] Besides the transfer of the entire E_n unit, its degradation as well as aggregation were also observed. Therefore, the question arises whether it would be possible to synthesize a related zirconium complex containing a polyantimony unit. Such derivative could be used to transfer the antimony entity to transition metals or main group compounds to build metastable polyantimony compounds. Herein we report on the successful synthesis of $[(Cp''Zr)_2(\mu,\eta^{1:1:1:1:1:1}\text{-}Sb_6)]$ (**1**) and its unprecedented use as transfer reagent for Sb_n species. Nevertheless, in comparison to P_n and As_n transfer reagents, one should keep in mind the lesser stability of Sb–Sb bonds during the transfer, due to the much lower E–E single bond energy.

Results and discussion

To discover a suitable starting material for transfer reactions, we investigated the reaction of $[Cp''_2ZrCl_2]$ with $KSb(SiMe_3)_2$, surprisingly leading to the formation of the polyantimony triple decker complex $[(Cp''Zr)_2(\mu,\eta^{1:1:1:1:1:1}\text{-}Sb_6)]$ (**1**) as the only isolable and identified product (Scheme 1). Compound **1** is well soluble in solvents such as *n*-pentane, toluene or THF, and is highly air- and light-sensitive. It decomposes rapidly, especially in solution, even at low temperatures (−80 °C) after few days. Therefore, the recorded ^1H NMR spectrum of **1** at r.t. reveals the expected signals for the Cp″ ligands, but also unidentified decomposition products. Also, in the mass spectrum of **1**, the molecular ion peak with a correct isotopic pattern was detected at m/z = 1267.61, beside some other peaks, corresponding to decomposition products.

Crystals of **1** suitable for single crystal X-ray diffraction analysis were obtained by storing a concentrated solution in dichloromethane or *n*-pentane at −30 °C. The molecular structure of **1** is depicted in Fig. 2.

The central structural core represents a chair-type Sb_6 unit attached to two [Cp″Zr] fragments in an $\eta^{1:1:1:1:1:1}$ fashion, leading to a cube-like Zr_2Sb_6 core. The Sb–Sb distances of 2.8381(7) Å to 2.8783(6) Å are in the range of a single bond and in good agreement with other polyantimony ligand complexes.[14,16–18,26] Complexes containing chair-like Sb_6 ligands are not known. The most related compounds are the boat-like *cyclo*-Sb_6^{4-} species in the Zintl ion $[(Cp^*Ru)_2(\mu,\eta^{4:2:2}\text{-}Sb_6)]^{2-}$ reported by B. Eichhorn *et al.*[10c] and the phosphine ligand stabilized compound $[(R_3P)_4Sb_6]^{4+}$ containing a bicyclic Sb_6 moiety.[10d] Otherwise, only organo-antimony compounds bearing organic substituents ($(RSb)_6$, R = C_6H_5, C_7H_7) were published.[26,27] Complexes containing chair-like or skew boat-like E_6 (E = P, Bi) moieties have also been reported.[28] The most related complex to **1**, $[(Cp^*Ti)_2(\mu,\eta^{1:1:1:1:1:1}\text{-}P_6)]$, was synthesized by the co-thermolysis of $[Cp^*Ti(CO)_2]$ with white phosphorus.[28a] This compound can be formally described as a lighter congener of **1**. Only a few examples of compounds containing antimony and zirconium are known so far, but organic substituents are attached to the antimony atoms.[29]

DFT calculations were performed at the B3LYP/def2-TZVP level of theory to elucidate the electronic structure and the nature of the Sb_6 ligand in **1**. The Wiberg Bond Indices (WBI) of the Zr–Sb bonds of 0.97 (in average) indicate a covalent nature of these bonds. This applies also to the Sb–Sb bonds with a slightly lower value of 0.84 (average), confirming the presence of single bonds within the Zr_2Sb_4 unit. The natural charge distribution shows a positive charge concentration on the *cyclo*-Sb_6 ligand (+0.48) and Zr (+0.11 each), while the negative charge is located on the Cp″ ligand (−0.35 each).

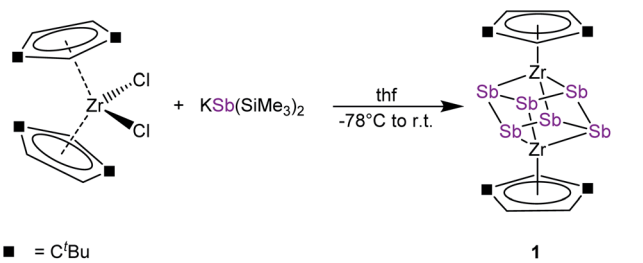

Scheme 1 Synthesis of **1**.

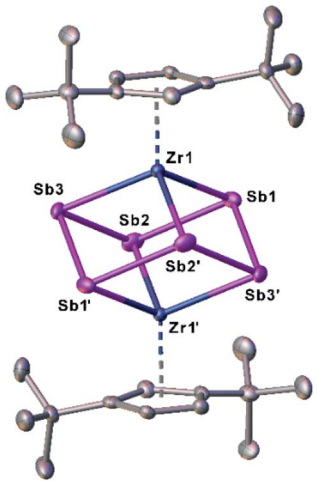

Fig. 2 Molecular structure of **1** in the solid state with thermal ellipsoids at 50% probability level. H atoms are omitted for clarity.

With compound **1** in hand, we investigated its suitability to transfer Sb_n units under mild conditions to late transition metals. For this purpose, transition metal halides of the type $[Cp'''MX]_2$ of nickel, cobalt and iron were used. The formation of the thermodynamically favored zirconium halogen bond represents the driving force of these reactions. Due to the very limited stability of **1**, *in situ* generated solutions were used under strict exclusion of light. All mentioned reactions were performed in THF at r.t. and a subsequent column chromatographic workup was needed for purifications, significantly reducing the yield of the formed products (*cf.* Scheme 2). The reaction of **1** with $[Cp'''NiBr]_2$ leads to $[(Cp'''Ni)_4(\mu_3\text{-}Sb)_4]$ (**2**), containing a cubane-like Ni_4Sb_4 core and the co-crystallization of nickelocene $[Cp'''_2Ni]$ (**2′**). Under similar reaction conditions, **1** reacts with $[Cp'''CoCl]_2$ exclusively to the heterocubane derivative $[(Cp'''Co)_4(\mu_3\text{-}Sb)_4]$ (**3a**). $[Cp^{Bn}CoCl]_2$, containing the sterically less encumbered Cp^{Bn} substituent, reacts with **1** to a mixture of $[(Cp^{Bn}Co)_4(\mu_3\text{-}Sb)_4]$ (**3b**) and $[(Cp^{Bn}Co)_3(\mu_3\text{-}Sb)_2]$ (**4**).[30] Despite numerous attempts, **3b** and **4** could not be separated to be obtained as analytically pure compounds. Furthermore, the reaction of **1** with $[Cp'''FeBr]_2$ leads to two products after chromatographic workup, $[(Cp'''Fe)_3(\mu_3\text{-}Sb)_2]$ (**5**) and $[(Cp'''Fe)_3(\mu_3,\eta^{4:4:4}\text{-}Sb_6)]$ (**6**). Whereas in the afore-reported products **2**, **3a**, **3b**, **4** and **5** only Sb_1 units are incorporated, in **6**, the complete Sb_6 entity was transferred. The ^1H and $^{13}C\{^1H\}$ NMR spectra of **2**/**2′** reveal the expected signals for **2**. Due to the paramagnetic nature of **2′**, no signals are detected in the diamagnetic region. ^1H NMR measurements of the mixture of **3b** and **4** show two sets of signals, which can be attributed to **3b** and **4**, respectively. Although **3b** is paramagnetic, the ^1H NMR signals occur in the diamagnetic region probably due to the strong localization of the spin density on the cobalt centers. Thus, the ratio between **3b** and **4** of 2 : 1 could be identified. In the ^1H NMR spectra of **3a**, **5** and **6**, only broad signals for the ^{t}Bu groups are observed, due to their paramagnetic character. The molecular ion peaks with the correct isotope pattern were detected for all mentioned compounds by mass spectrometry.[31]

Single crystals of **2**/**2′** and **3a** suitable for crystal X-ray diffraction analysis were obtained by layering a toluene solution with acetonitrile (**2**/**2′**) or by storing a concentrated *n*-hexane solution at −30 °C (**3a**) (Fig. 3). Surprisingly, **2** co-crystallizes with **2′** in a ratio of 2 : 1 (ESI: Fig. S2†). The central structural core of **2** and **3a** consists of a distorted heterocubane unit built up by four nickel or cobalt and four antimony atoms (Fig. 3). The square faces of the cubanes show a kite-like distortion in which the Sb atoms approach each other. All nickel and cobalt atoms are coordinatively saturated by the coordination of a Cp‴ ligand. The Ni–Sb bond lengths in **2** (2.5202(7) Å to 2.5602(7) Å)[32,33] and the Co–Sb bond lengths in **3a** (2.5023(19) Å to 2.6305(14) Å)[12,34–37] are in the range of corresponding single bonds. While, in **2**, the Ni–Ni distances are quite long (3.9352(9) Å to 3.962(1) Å) indicating no bonding interaction, in **3a**, there are two short Co···Co distances of 3.071(4) Å and two long Co···

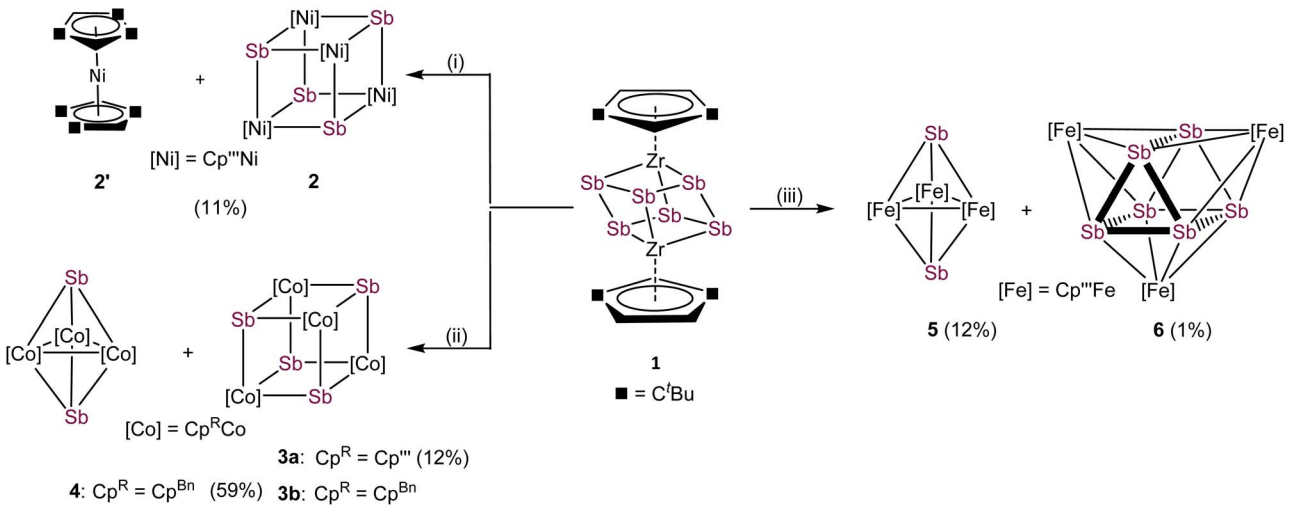

Scheme 2 Reaction of *in situ* prepared $[(Cp''Zr)_2(\mu,\eta^{1:1:1:1:1:1}\text{-}Sb_6)]$ (**1**) with transition metal halides at r.t. in THF. (i): **1** with $[Cp'''NiBr]_2$; (ii): **1** with $[Cp^RCoCl]_2$ ($Cp^R = Cp^{Bn}$, Cp‴); (iii): **1** with *in situ* prepared $[Cp'''FeBr]_2$: isolated yields are given in parentheses.

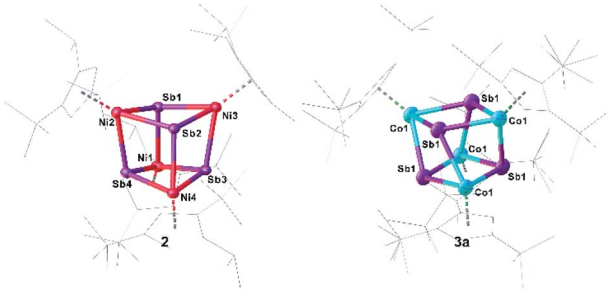

Fig. 3 Molecular structures of **2** (left) and **3a** (right) in the solid state with thermal ellipsoids at 50% probability level. H atoms are omitted and the Cp‴ ligands drawn in the *wire* frame model for clarity.

Co distances of 4.034(3) Å. Similarly, the Sb–Sb distances in **2** are reasonably similar (3.0767(4) Å to 3.1613(4) Å), while, in **3a**, there are two very short (2.9453(13) Å) and two longer (3.1763(13) Å) Sb–Sb distances. The former lies in the range of an elongated single bond.[38] The distortion of the M_4Sb_4 core is more accentuated in **3a** than in **2**, probably due to the Co⋯Co and Sb⋯Sb interactions. The rhombic distortion of the cubanes $[(Cp^*M)_4E_4]$ (M = Cr, Mo, E = O, S) was attributed to ferromagnetic as well as antiferromagnetic couplings of the metal-based electrons.[39]

DFT calculations reproduce well the geometric parameters of the model compound $[(Cp^*Co)_3(\mu\text{-}Sb)_2]$ (**4m**; *vide infra*), while the short Co–Co distances in **3a** are slightly longer in the optimized geometry, irrespective of a singlet or a triplet spin state. The short Sb–Sb distances in **3a** are well reproduced. The presence of Sb⋯Sb interactions in **2** and **3a** are substantiated by the Mayer bond orders, which vary from 0.25 to 0.35 and from 0.27 to 0.52, respectively correlate with the corresponding distances. Based on the analysis of the Intrinsic Bonding Orbitals,[40] the Co⋯Co interaction in **3m** is realized *via* the Co–Sb σ-bond to which contributions of roughly 10% from the other two Co atoms are mixed. Additionally, on each Co center, there are three non-bonding d orbitals which do not overlap to give Co–Co bonds. The Mayer bond order for the Co–Co interactions in **4m** is roughly 0.48 while for the Co–Sb bonds vary from 0.92 to 0.98. To investigate the electronic structure of **3a** in more detail, EPR and Evans NMR investigations were performed. **3a** is EPR-silent and has an effective magnetic moment of $\mu_{eff} = 2.34\ \mu_B$, corresponding roughly to two unpaired electrons as determined by the Evans method.[41]

Compounds **4** and **5** crystallize as brown and violet blocks, respectively, by layering a toluene solution with acetonitrile. Their central structural motif consists of an $[M_3Sb_2]$ trigonal bipyramide, built up by two antimony and three metal atoms (M = Co (**4**), Fe (**5**), Fig. 4). The cobalt and iron atoms are located in the equatorial plane and coordinated by a Cp^R ligand, the antimony atoms occupy the apical positions. While the Fe–Sb distances of 2.4895(6) Å to 2.55342(5) Å are in good agreement with reported single bonds,[1,42,43] the Co–Sb distances of **4** (2.4362(4) Å to 2.4547(4) Å) are shortened.[12,34–37] A remarkable difference between the geometry of **4** and **5** is represented by the M–M distances. While, in **4**, the Co–Co distances are all very similar (2.7284(6) Å to 2.7332(5) Å) and lie in the same range of elongated single bonds,[33,43] in **5**, there are one short (2.4489(6) Å and 2.4895(6) Å) and two longer Fe–Fe distances (2.8076(6) Å to 2.9230(6) Å).[44] Interestingly, the nitrogen congener of **5**, $[(Cp'''Fe)_3(\mu_3\text{-}N)_2]$, possesses uniform Fe–Fe distances varying from 2.4727(4) Å to 2.4734(4) Å,[45] while the phosphorus and arsenic derivatives $[(Cp^*Fe)_3(\mu_3\text{-}E)_2]$ (E = P, As)[46] show a distortion of the Fe_3 fragment that is similar to **5**, but less accentuated. The structure of **4** represents a new structural motif and can be regarded as a *closo*-type cluster with 12 skeletal electrons according to the Wade-Mingos rule. Similar complexes of iron and antimony are known only for antimony atoms coordinating to Lewis acidic metal fragments as in $[Fe_3(CO)_9(\mu_3\text{-}SbML_n)_2]$ (ML_n = $CpMn(CO)_2$, $Cr(CO)_5$, $W(CO)_5$, $Mo(CO)_5$).[1,42]

To explore the electronic structure of **5**, EPR and Evans NMR investigations were performed. The X-band EPR spectrum of **5** at 77 K in frozen toluene shows an axial signal ($g_x = g_y = 2.177$ and $g_z = 2.443$ ($g_{iso} = 2.266$)) with no hyperfine splitting (Fig. 5). The doublet spin state of **5** is further supported by Evans NMR measurements, resulting in $\mu_{eff} = 1.65\ \mu_B$, corresponding roughly to one unpaired electron.[41]

In order to elucidate the electronic structure of **5**, DFT calculations were performed. The geometry of **5** in different spin states (S = 1/2 to 4) was optimized by using different

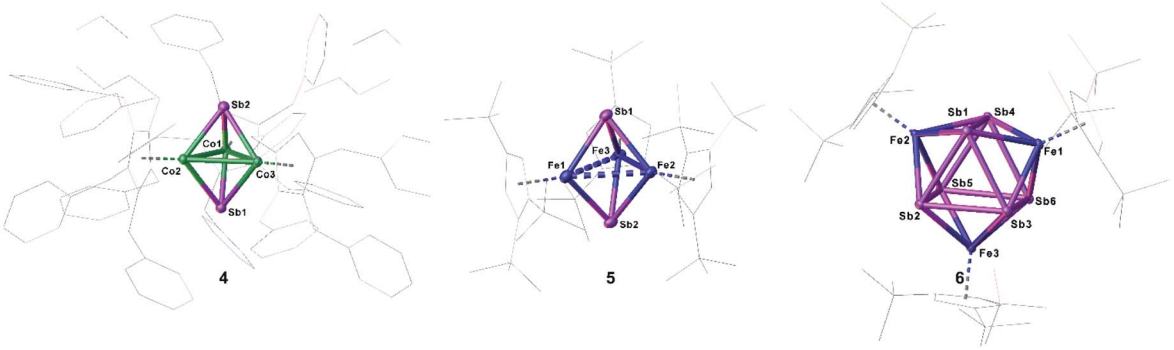

Fig. 4 Molecular structures of **3b** (left), **5** (middle) and **6** (right) in the solid state with thermal ellipsoids at 50% probability level. H atoms are omitted and the Cp‴ ligands drawn in the *wire* frame model for clarity.

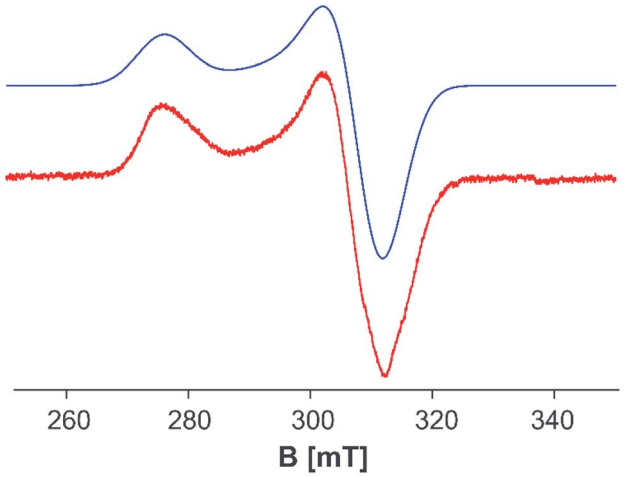

Fig. 5 X-band EPR spectrum of **5** in toluene at 77 K: $g_x = g_y = 2.177$ and $g_z = 2.443$ ($g_{iso} = 2.266$). Red: experimental; blue: simulated.[47]

functionals. The results show that only the OPBE functional in a doublet spin state reproduces the experimental geometry of **5** found in the solid state. Hybrid functionals lead to optimized geometries with considerably longer Fe–Fe distances, while a similar trend is observed for the OPBE functional in higher spin states (*cf.* ESI†). Single point calculations with both functionals OPBE and B3LYP (OPBE, doublet spin state optimized geometry) predict the doublet spin state as the energetically lowest state, while the other spin states lie energetically higher (*cf.* ESI†). Therefore, the ground state of **5** can be viewed as being a doublet spin state, which is in accordance with the EPR and Evans NMR data (*vide supra*). For the nitrogen analog of **5**, $[(Cp'''Fe)_3(\mu_3\text{-}N)_2]$, the presence of three low-spin iron(III) ($S = 1/2$) centers and a total spin of $S_{tot} = 1/2$ was reported, due to complex antiferromagnetic coupling.[45]

Single crystals of **6** suitable for X-ray diffractions were obtained after chromatographic workup by layering a toluene solution with acetonitrile. The central structural motif of **6** consists of a Sb_6 prism with its rectangular faces being capped by [Cp‴Fe] fragments (Fig. 4, right). Within the triangular faces, the Sb–Sb distances (2.9029(4) Å to 2.9365(4) Å) are slightly shorter than the Sb–Sb distances between them (3.0283(4) Å to 3.0646(4) Å). This variation of the Sb–Sb distances nicely correlates with the corresponding Mayer bond orders (OPBE/def2-SVP, doublet spin state) of 0.53 and 0.33, respectively. The Mayer bond orders for the Fe–Sb bonds vary only slightly between 0.69 to 0.73. Although the Sb–Sb distances are slightly longer than usual Sb–Sb single bonds, they lie in the range of elongated single bonds.[14,16,18,48] DFT calculations at the OPBE/def2-SVP level predict the doublet spin state for **6** as ground state, with the spin density being evenly distributed over the three Fe centers, while the other spin states lie energetically higher (for example the quartet spin state is with 53 kJ mol^{-1} higher in energy; *cf.* ESI†). To the best of our knowledge, **6** is the first complex containing a Sb_6 prism. Comparable complexes are only known for other group 15 homologous.[49]

Conclusions

In summary, we herein report the synthesis of the first zirconium antimony ligand complex $[(Cp''Zr)_2(\mu,\eta^{1:1:1:1:1:1}\text{-}Sb_6)]$ (**1**), which contains an unprecedented chair-like Sb_6 ligand coordinated to two Cp″Zr fragments. Complex **1** can be used as an effective antimony transfer reagent towards transition metal halides of nickel, cobalt and iron. That way, a variety of novel Sb_n ligand complexes such as the cubane-like compounds $[(Cp'''Ni)_4(\mu_3\text{-}Sb)_4]/[Cp'''_2Ni]$ (**2**/**2′**) and $[(Cp'''Co)_4(\mu_3\text{-}Sb_4)]$ (**3a**) or the complexes $[(Cp^{Bn}Co)_3(\mu_3\text{-}Sb)_2]$ (**4**) and $[(Cp'''Fe)_3(\mu_3\text{-}Sb)_2]$ (**5**) containing a trigonal bipyramidal structure were obtained and fully characterized. Beside the partial transfer of the Sb_1 units, also the complete transfer of a Sb_6 unit was achieved. Here, the iron complex $[(Cp'''Fe)(\mu,\eta^{4:4:4}\text{-}Sb_6)]$ (**6**) is formed which shows the potential of **1** as transfer reagent for polyantimony units. In principle, an initial transfer of larger Sb_n units from **1** should have been possible, however, the low stability of such complexes (especially during column chromatographic work-up) might be the reason that mostly only Sb_1-unit-containing complexes were isolated. Future work in this area is dedicated to developing smoother reaction pathways.

Data availability

Crystallographic data for **1**–**6** has been deposited at the CCDC/ICSD under 2079755 (**1**), 2079756 (**2**/**2′**), 2079757 (**3a**), 2079758 (**4**·C_7H_8), 2079759 (**5**) and 2079760 (**6**).

Author contributions

Veronika Heinl, synthesis and characterization of compounds **2**, **3a**, **5** and **6** and writing the paper. Dr Andreas E. Seitz, synthesis and characterization of compounds **1**, **3b** and **4**. Dr Michael Seidl, recalculating the X-ray structures. Dr Gábor Balázs, computational details. Manfred Scheer, supervising the whole research work, fund raising and writing the paper. All authors have read and agreed to the published version of the manuscript.

Conflicts of interest

There are no conflicts to declare.

Acknowledgements

The Deutsche Forschungsgemeinschaft within the project Sche 384/32-2 supported this work. V. Heinl is grateful to the Fonds der Chemischen Industrie for a PhD fellowship.

Notes and references

1 B. E. Collins, Y. Koide, C. K. Schauer and P. S. White, *Inorg. Chem.*, 1997, **36**, 6172–6183.
2 C. M. Hoidn, D. J. Scott and R. Wolf, *Chem.–Eur. J.*, 2021, **27**, 1886–1920.

3 (*a*) M. Caporali, L. Gonsalvi, A. Rossin and M. Peruzzini, *Chem. Rev.*, 2010, **110**, 4178–4235; (*b*) F. Scalambra, M. Peruzzini and A. Romerosa, *Adv. Organomet. Chem.*, 2019, 173–222; (*c*) N. A. Giffin and J. D. Masuda, *Coord. Chem. Rev.*, 2011, **255**, 1342–1359; (*d*) O. J. Scherer, *Acc. Chem. Res.*, 1999, **32**, 751–762.

4 B. M. Cossairt, N. A. Piro and C. C. Cummins, *Chem. Rev.*, 2010, **110**, 4164–4177.

5 L. Qiao, C. Zhang, X. W. Zhang, Z. C. Wang, H. Yin and Z. M. Sun, *Chin. J. Chem.*, 2020, **38**, 295–304.

6 M. Scheer, G. Balázs and A. Seitz, *Chem. Rev.*, 2010, **110**, 4236–4256.

7 (*a*) O. J. Scherer, *Angew. Chem., Int. Ed. Engl.*, 1985, **24**, 924–943; (*b*) O. J. Scherer, *Angew. Chem., Int. Ed. Engl.*, 1990, **29**, 1104–1122.

8 Y. R. Luo, *Comprehensive Handbook of Chemical Bond Energies*, CRC Press, Boca Raton, 2007.

9 (*a*) J. Kordis and K. A. Gingerich, *J. Chem. Phys.*, 1973, **58**, 5141–5149; (*b*) J. Mühlbach, P. Pfau, E. Recknagel and K. Sattler, *Surf. Sci.*, 1981, **106**, 18–26; (*c*) V. E. Bondybey, G. P. Schwartz and J. E. Griffiths, *J. Mol. Spectrosc.*, 1981, **89**, 328–332; (*d*) R. Prasad, V. Venugopal, Z. Singh and D. D. Sood, *J. Chem. Thermodyn.*, 1979, **11**, 963–970; (*e*) H. Zhang and K. Balasubramanian, *J. Chem. Phys.*, 1992, **97**, 3437–3444.

10 (*a*) S. Scharfe, F. Kraus, S. Stegmaier, A. Schier and T. F. Fässler, *Angew. Chem., Int. Ed.*, 2011, **50**, 3630–3670; (*b*) R. S. P. Turbervill and J. M. Goicoechea, *Chem. Rev.*, 2014, **114**, 10807–10828; for the use of K3Sb *cf.*: (*c*) Y. Wang, P. Zavalij and B. Eichhorn, *Chem. Commun.*, 2018, **54**, 11917–11920; (*d*) S. S. Chitnis, N. Burford, J. J. Weigand and R. McDonald, *Angew. Chem., Int. Ed.*, 2015, **54**, 7828–7832.

11 H. J. Breunig, *Organic Arsenic, Antimony and Bismuth Compounds* 1994, John Wiley & Sons, pp. 563–577.

12 L. F. Dahl and A. S. Foust, *J. Am. Chem. Soc.*, 1970, **92**, 7337–7341.

13 G. Huttner, U. Weber, B. Sigwarth and O. Schneidsteger, *Angew. Chem., Int. Ed. Engl.*, 1982, **21**, 215–216.

14 L. Tuscher, C. Ganesamoorthy, D. Bläser, C. Wölper and S. Schulz, *Angew. Chem., Int. Ed.*, 2015, **54**, 10657–10661.

15 H. J. Breunig, R. Rösler and E. Lork, *Angew. Chem., Int. Ed. Engl.*, 1997, **36**, 2819–2821.

16 H. J. Breunig, N. Burford and R. Rösler, *Angew. Chem., Int. Ed.*, 2000, **39**, 4148–4150.

17 C. Ganesamoorthy, J. Krüger, C. Wölper, A. S. Nizovtsev and S. Schulz, *Chem.–Eur. J.*, 2017, **23**, 2461–2468.

18 C. Ganesamoorthy, C. Wölper, A. S. Nizovtsev and S. Schulz, *Angew. Chem., Int. Ed.*, 2016, **55**, 4204–4209.

19 (*a*) Y. Wang, P. Zavalij and B. Eichhorn, *Chem. Commun.*, 2018, **54**, 11917–11920; (*b*) C. Ganesamoorthy, C. Helling, C. Wölpe, W. Frank, E. Bill, G. E. Cutsail and S. Schulz, *Nat. Commun.*, 2018, **9**, 87; (*c*) C. Schoo, S. Bestgen, A. Egeberg, S. Klementyeva, C. Feldmann, S. N. Konchenko and P. W. Roesky, *Angew. Chem., Int. Ed.*, 2018, **57**, 5912–5916; (*d*) C. Helling, C. Wölper and S. Schulz, *Dalton Trans.*, 2020, **49**, 11835–11842; (*e*) C. Helling, G. E. Cutsail, H. Weinert, C. Wölper and S. Schulz, *Angew. Chem., Int. Ed.*, 2020, **59**, 7561–7568.

20 C. Schoo, S. Bestgen, A. Egeberg, S. Klementyeva, C. Feldmann, S. N. Konchenko and P. W. Roesky, *Angew. Chem., Int. Ed.*, 2018, **57**, 5912–5916.

21 G. Balázs, M. Sierka and M. Scheer, *Angew. Chem., Int. Ed.*, 2005, **44**, 4920–4924.

22 T. Wetting, B. Geissler, R. Schneider, S. Barth, P. Binger and M. Regitz, *Angew. Chem., Int. Ed. Engl.*, 1992, **31**, 758–759.

23 B. M. Cossairt, M.-C. Diawara and C. C. Cummins, *Science*, 2009, **323**, 602.

24 A. E. Seitz, M. Eckhardt, A. Erlebach, E. V. Peresypkina, M. Sierka and M. Scheer, *J. Am. Chem. Soc.*, 2016, **138**, 10433–10436.

25 M. Schmidt, A. E. Seitz, M. Eckhardt, G. Balázs, E. V. Peresypkina, A. V. Virovets, F. Riedlberger, M. Bodensteiner, E. M. Zolnhofer, K. Meyer and M. Scheer, *J. Am. Chem. Soc.*, 2017, **139**, 13981–13984.

26 H. J. Breunig, K. Häberle, M. Dräger and T. Severengiz, *Angew. Chem., Int. Ed. Engl.*, 1985, **24**, 73.

27 H. J. Breunig, K. H. Ebert, S. Gülec and J. Probst, *Chem. Ber.*, 1995, **128**, 599–603.

28 (*a*) O. J. Scherer, H. Swarowsky, G. Wolmershäuser, W. Kaim and S. Kohlmann, *Angew. Chem., Int. Ed. Engl.*, 1987, **26**, 1153–1155; (*b*) J. M. Goicoechea, M. W. Hull and S. C. Sevov, *J. Am. Chem. Soc.*, 2007, **129**, 7885–7893; (*c*) H.-G. von Schnering, M. Wittmann and R. Nesper, *J. Less Common Met.*, 1980, **76**, 213–226.

29 (*a*) S. R. Wade, M. G. H. Wallbridge and G. R. Willey, *J. Organomet. Chem.*, 1984, **267**, 271–276; (*b*) R. Zitz, J. Baumgartner and C. Marschner, *Organometallics*, 2015, **34**, 1431–1439.

30 Despite several attempts, it was not possible to structurally identify **3a**. Its composition and structure are assigned based on mass spectrometric data and are presumably isostructural to the cubanes **2** and **3b**.

31 Note that the peak for **3b** is relatively weak presumably due to its high mass (2785 Da).

32 (*a*) P. D. Mlynek and L. F. Dahl, *Organometallics*, 1997, **16**, 1641–1654; (*b*) S. Charles, B. W. Eichhorn and S. G. Bott, *J. Am. Chem. Soc.*, 1993, **115**, 5837–5838.

33 U. Vogel, G. Baum and M. Scheer, *Z. Anorg. Allg. Chem.*, 2000, **626**, 444–449.

34 T. A. Albright, K. A. Yee, J. Y. Saillard, S. Kahlal, J. F. Halet, J. S. Leigh and K. H. Whitmire, *Inorg. Chem.*, 1991, **30**, 1179–1190.

35 N. C. Norman, P. M. Webster and L. J. Farrugia, *J. Organomet. Chem.*, 1992, **430**, 205–219.

36 J. S. Leigh, K. H. Whitmire, K. A. Yee and T. A. Albright, *J. Am. Chem. Soc.*, 1989, **111**, 2726–2727.

37 S. N. Konchenko, A. V. Virovets, S. A. Apenina and S. V. Tkachev, *Inorg. Chem.*, 1999, 555–557.

38 P. Pyykkö and M. Atsumi, *Chem.–Eur. J.*, 2009, **15**, 186–197.

39 J. E. McGrady, *J. Chem. Soc., Dalton Trans.*, 1999, 1393–1399.

40 G. Knizia, *J. Chem. Theory Comput.*, 2013, **9**, 4834–4843.

41 Due to the high molecular weight and bad solubility, the results of the Evans NMR should be treated with care.

42 H. Lang, G. Huttner, L. Zsolnai, G. Mohr, B. Sigwarth, U. Weber, O. Orama and I. Jibril, *J. Organomet. Chem.*, 1986, **304**, 157–179.
43 T. Gröer, T. Palm and M. Scheer, *Eur. J. Inorg. Chem.*, 2000, 2591–2595.
44 There are two different bond distances due to two molecules in the asymmetric unit.
45 M. Reiners, D. Baabe, K. Münster, M.-K. Zaretzke, M. Freytag, P. G. Jones, Y. Coppel, S. Bontemps, I. D. Rosal, L. Maron and M. D. Walter, *Nat. Chem.*, 2020, **12**, 740–746.
46 S. Reisinger, Organometallic Pnictogen Chemistry – Three Aspects, PhD thesis, University of Regensburg, 2014.
47 S. Stoll and A. Schweiger, *J. Magn. Reson.*, 2006, **178**, 42–55.
48 H. J. Breunig, R. Rösler and E. Lork, *Angew. Chem., Int. Ed. Engl.*, 1997, **36**, 2819–2821.
49 (*a*) S. Heinl, A. Y. Timoshkin, J. Müller and M. Scheer, *Chem. Commun.*, 2018, **54**, 2244–2247; (*b*) C. Hänisch, D. Fenske, F. Weigend and R. Ahlrichs, *Chem.–Eur. J.*, 1997, **3**, 1494–1498; (*c*) C. Hänisch, D. Fenske, F. Weigend and R. Ahlrichs, *Chem.–Eur. J.*, 1997, **3**, 1494–1498; (*d*) G. Friedrich, O. J. Scherer and G. Wolmershäuser, *Z. Anorg. Allg. Chem.*, 1996, **622**, 1478–1486; (*e*) L. Qiao, D. Chen, J. Zhu, A. Muñoz-Castro and Z.-M. Sun, *Chem. Commun.*, 2021, **57**, 3656–3659.